

Cite this: *Phys. Chem. Chem. Phys.*, 2011, **13**, 19206–19213

www.rsc.org/pccp

PERSPECTIVE

## Dynamics of reactions between two closed-shell molecules

Jim J. Lin\*<sup>abc</sup>

Received 15th July 2011, Accepted 6th September 2011

DOI: 10.1039/c1cp22305d

The crossed molecular beam technique has been utilized to investigate a large number of elementary reactions. However, most of the studied reactions involve atoms or radicals; reactions between two stable molecular reactants are, in fact, seldom studied with the crossed molecular beam method. In this perspective, reactions between two stable molecules are reviewed and discussed. With crossed molecular beams and vacuum UV photoionization, the nascent products have been unambiguously identified. Consistent pictures of the reaction paths have been constructed based on the experimental data and *ab initio* calculations. Furthermore, there are intriguing features about the reaction barriers. The  $F_2$  + organosulfur reactions are barrierless, demonstrating the first examples of such interactions between two closed-shell reactants. The barrier of  $F_2$  + alkene reaction decreases with more methyl substitution groups at the  $C=C$  double bond, yet the absolute barrier heights from experiment and theory disagree with each other by  $\sim 2$  kcal mol $^{-1}$ , leaving an issue to be resolved in the future.

### 1. Introduction

Crossed molecular beam reactive scattering has been a powerful tool to study dynamics of elementary chemical reactions.<sup>1–11</sup> This technique is most suitable when one would like to (i) control the energies of the reagents, (ii) understand the dependence of chemical reactivity on molecular orientation, (iii) explore the nature of reaction intermediates and their subsequent decay dynamics, and (iv) identify complex reaction mechanisms. However, the vast majority of the reactions which have been investigated with the crossed molecular beam technique are atom–molecule or radical–molecule reactions.<sup>1–11</sup> To the best of our knowledge, only a very limited number of molecule–molecule reactions<sup>12–19</sup> had been studied with crossed molecular beams before 2007. Even some radical–radical reactions have been investigated with this technique.<sup>20–25</sup> Therefore, it is natural to wonder about the dynamics of molecule–molecule reactions. Herein we call a chemical species with open-shell electronic structure a *radical* and a species with closed-shell electronic structure a *molecule*. In this terminology, a molecule is often believed to be more stable than a radical; in comparison with radical reactions, smaller rate constants and higher activation energies may be expected for reactions between two molecules. On the other hand, it would be interesting to learn if there are any exceptions.

After decades of investigations, quite a few reaction mechanisms,<sup>2,3</sup> such as abstraction, addition, association, insertion, *etc.*, have been reasonably well studied and established for many radical reactions. In contrast, studies on molecule–molecule reactions are very sparse. Before our works,<sup>26–31</sup> reactions of molecular fluorine with  $I_2$ ,  $ICl$ ,  $HI$ ,  $CH_3I$ , and  $C_6H_6$  had been investigated with crossed molecular beams;<sup>12–19</sup> considerable collision energies ( $\sim 4, 6, 11, 11, \text{ and } 14$  kcal mol $^{-1}$ , respectively) are required to promote the reactions and only a  $F$  atom and a fluoro radical were observed as the products. The authors<sup>12–19</sup> concluded that the newly formed  $F-X$  bond is weaker than the  $F-F$  bond of  $F_2$  ( $F-F + X \rightarrow F-X + F$ ;  $X$  denotes the  $I_2$ ,  $ICl$ ,  $HI$ ,  $CH_3I$ , or  $C_6H_6$  reactant), such that a certain amount of collision energy is required for product formation.

Recently, our group<sup>26–31</sup> has managed to study a few molecule–molecule reactions with the crossed molecular beam technique. Two types of reactions have been investigated: the first one is reaction of  $F_2$  with organosulfur molecules<sup>26–28</sup> and the other is reaction of  $F_2$  with alkene molecules.<sup>29–31</sup> These results reveal new information which would enhance our understanding of chemical reactivity and broaden our chemical intuition.

Until now, the studied crossed beam reactions between two molecules have all involved molecular fluorine. Fluorine gas is often thought to be quite reactive, but it should be clarified whether the high reactivity is from  $F_2$  molecules or from  $F$  atoms which may be produced after some radical initiation processes. For example, a mixture of  $F_2$  and  $H_2$  gases will form  $HF$ . But the elementary reaction of  $F_2 + H_2$  is very slow and has a high activation energy; the main chemical processes to produce  $HF$  usually involve radicals and/or surfaces. Hereafter, we will focus our discussion on primary processes between two molecules, not on secondary reactions.

<sup>a</sup> Institute of Atomic and Molecular Sciences, Academia Sinica, Taipei 10617, Taiwan. E-mail: jimlin@gate.sinica.edu.tw;  
Fax: +886-2-23620200

<sup>b</sup> Department of Applied Chemistry, National Chiao Tung University, Hsinchu 30010, Taiwan

<sup>c</sup> Department of Chemistry, National Taiwan University, Taipei 10617, Taiwan

## 2. Experimental

Crossed molecular beam experiments are quite different from bulk experiments. In particular, reaction products can accumulate in bulk, not in crossed beam conditions. The “price” for observing nascent products under single collisions is that the number of product molecules is usually much smaller than the numbers of the reactants, because the reaction cross section is usually much smaller than the non-reactive (elastic and inelastic) scattering cross sections. For crossed molecular beam experiments with mass spectrometry detection,<sup>32–36</sup> if we probe the non-reactive scattering events at the reactant masses, the signal level is often several orders of magnitude higher than that of the reaction products. Therefore, the success of a reactive scattering experiment heavily relies on non-overlapping between the product and reactant masses. Although a molecular beam of a stable species can reach a much higher intensity compared to a radical beam (the density of a radical beam is limited by a few natural processes like radical recombination), background from the non-reactive scattering would be large, which may cause difficulties in detecting the relatively weaker signal of the reaction products.

Pulsed molecular beams were chosen in our experiments to have a better signal-to-noise ratio (see Appendix). The crossing angle in our apparatus was fixed at 90°. Typically we utilized supersonic expansion to produce a molecular beam with a speed distribution of about  $\pm 5\%$ . The resulting spread in collision energy was about  $\pm 10\%$ . The mean speed of a molecular beam was adjusted either by changing the seeding ratio in various rare gases or by changing the nozzle temperature. After two reactant beams crossed, the scattered neutral products flew to the mass spectrometry detector. Time-of-flight (TOF) spectra of the scattering events were then recorded at selected  $m/z$  values and laboratory angles. The laboratory-frame velocity and angular distributions of the products were obtained from the TOF spectra at a number of laboratory angles and converted to the center-of-mass frame by a forward convolution routine.

Two apparatuses were used for these investigations. The synchrotron radiation (SR) machine<sup>34,35</sup> consists of rotatable sources and a fixed mass detector with vacuum UV photoionization. The electron-impact-ionization (EI) machine<sup>32</sup> consists of fixed sources and a rotatable mass detector with electron-impact ionization. The product flight path of the EI machine was about 24.5 cm, significantly longer than the 10 cm of the SR machine. Because the synchrotron beamtime was limited, the main results were obtained from the EI machine which also offered a better TOF resolution. The SR machine was mainly used to measure the photoionization efficiency spectra of the reaction products.

For molecule–molecule reactive scattering, we define the forward/backward directions of a probed product as follows. Assume a symbolized reaction of  $A + BC \rightarrow AB + C$ , where A, B and C can be atoms or groups of atoms. If AB is detected, we define its forward direction as the direction of A in the center-of-mass frame. Following this definition, a rebound reaction<sup>2</sup> would have a backward angular distribution for the detected product.

## 3. $F_2$ + organosulfur reactions

Turnipseed and Birks<sup>37</sup> reported significant reactivity of  $F_2$  towards organo-sulfur, -selenium, -tellurium, -phosphorous,

and -arsenide compounds, while most hydrocarbons, alcohols, or ethers give no reaction. Their observation is very interesting but we felt that the product identifications and reaction mechanisms were not clear at all by their flow-tube data. Therefore, we chose to study  $F_2$  reactions with dimethyl sulfide (DMS,  $CH_3SCH_3$ ) and dimethyl disulfide (DMDS,  $CH_3SSCH_3$ ) to learn more about the reaction dynamics.

Because  $F_2$  has a high electron affinity of about 3.0 eV, Turnipseed and Birks<sup>37</sup> also speculated that these reactions are initiated by the transfer of an electron from the organic molecule (DMS, DMDS, *etc.*) to  $F_2$ , similar to a “harpoon” mechanism<sup>2</sup> observed in reactions between alkali metal atoms and halogen compounds. The harpoon mechanism describes that the interaction involves a crossing between the ion-pair potential energy surface and the neutral potential energy surface. With the ionization energy of DMS (8.7 eV), a critical distance of the crossing can be estimated<sup>27</sup> to be 2.5 Å for the  $F_2 + DMS$  reaction by assuming point charges of the ion pair and a flat potential energy surface of the neutral system. However, this critical distance is significantly shorter than the sum of the van der Waals radii of F and S atoms (3.3 Å.  $R_{VDW}(S) = 1.8 \text{ \AA}$ ,  $R_{VDW}(F) = 1.5 \text{ \AA}$ ). This analysis indicates that to reach the hypothetical crossing point, the reactant molecules would need to be “squeezed” together, which requires energy. However, as will be shown later, the  $F_2$  reactions with DMS and DMDS are essentially barrierless.<sup>26–28</sup> Although Turnipseed and Birks<sup>37</sup> found a strong negative correlation between the ionization energies of a few organic reactants and their reactivity towards  $F_2$ , the harpoon mechanism is not enough to describe the reactions after taking a closer look.

### 3.1 $F_2$ + $CH_3SCH_3$ reaction

After crossing the reactant beams of  $F_2$  and  $CH_3SCH_3$ , TOF signals could be obtained at  $m/z = 80$  ( $C_2H_5SF^+$ ) and 81 ( $C_2H_6SF^+$ ).<sup>26,27</sup> To make sure that the signals were indeed from the  $F_2 + DMS$  reaction, we performed a blank experiment of Ar + DMS scattering under very similar experimental conditions. We also found that the signal of non-reactive scattering is similar for DMS +  $F_2$  and DMS + Ar by detecting the TOF spectra of the scattered DMS molecules. By comparing the scattering signals of DMS with  $F_2$  and Ar, we realized that some of the signals at  $m/z = 80$  and 81 were from impurity in the DMS molecular beam which was scattered by both  $F_2$  and Ar beams. This type of background cannot be measured with conventional beam modulation methods. After some efforts of chemical purification, the background was reduced but still noticeable. Finally we managed to eliminate this interference by changing the DMS sample to deuterium-substituted DMS or a DMS sample from a new supplier (Aldrich).

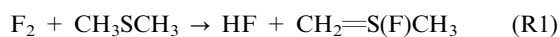
In multiple collision experiments, it is often difficult to identify nascent products due to secondary reactions. The situation is more severe for the  $F_2 + DMS$  reaction, because the F atom product is much more reactive than the  $F_2$  reactant<sup>38</sup> (by 1 to 2 orders of magnitude). As mentioned by Turnipseed and Birks,<sup>37</sup> “. . . due to the large variety of possible products, it is not possible to isolate any distinct reaction steps under these conditions.” Table 1 lists the experimental observations of the reaction products of  $F_2 + DMS$  studied under flow

**Table 1** Experimental observations of the reaction products of F<sub>2</sub> + CH<sub>3</sub>SCH<sub>3</sub> studied under flow tube and crossed beam conditions

Reference	Reaction condition	Detection method <sup>a</sup>	Assigned product(s)	Comment
Turnipseed and Birks <sup>37</sup>	Fast flow tube	IR emission Titration EI-MS	HF, H <sub>2</sub> CS, HCF F <i>m/z</i> = 80 (CH <sub>2</sub> =S(F)CH <sub>3</sub> )	Secondary products <i>via</i> Cl <sub>2</sub> + F → ClF + Cl The structure assignment was tentative
Baker <i>et al.</i> <sup>39</sup>	Fast flow tube	PES	VIE = 8.0 eV (CH <sub>3</sub> -S(F)-CH <sub>3</sub> ) H <sub>2</sub> CS, H <sub>2</sub> CCS, CH <sub>3</sub> SH, HFCS, HCF	Only at early reaction times Secondary products
Lu <i>et al.</i> <sup>26,27</sup>	Crossed beams	EI-MS VUV PI-MS	<i>m/z</i> = 80 (C <sub>2</sub> H <sub>5</sub> SF) + <i>m/z</i> = 20 (HF) <i>m/z</i> = 81 (C <sub>2</sub> H <sub>6</sub> SF) + <i>m/z</i> = 19 (F) CH <sub>2</sub> =S(F)CH <sub>3</sub> (VIE = 8.7 eV) + HF CH <sub>3</sub> -S(F)-CH <sub>3</sub> (VIE = 7.8 eV) + F	Confirmed with <i>ab initio</i> calculation of reaction paths Confirmed with <i>ab initio</i> calculation of IE

<sup>a</sup> EI-MS = electron-impact ionization mass spectrometry; PES = photoelectron spectroscopy; PI-MS = photoionization mass spectrometry.

tube and crossed beam conditions. Quite a few secondary products have been observed in the flow tube experiments.<sup>37,39</sup> With the crossed molecular beam technique, two primary product channels have been unambiguously identified:<sup>26,27</sup>



( $\Delta H_{0\text{K}}^\circ(\text{R1}) = -80.1 \text{ kcal mol}^{-1}$ ,  $\Delta H_{0\text{K}}^\circ(\text{R2}) = +3.4 \text{ kcal mol}^{-1}$ , both from CCSD(T) computations.)<sup>27</sup> The major product channel is (R1); (R2) is endothermic and was observed only at collision energies higher than 6 kcal mol<sup>-1</sup>. The measured kinetic energy releases of (R1) and (R2) are also consistent with the reaction enthalpies.<sup>27</sup>

The ionization energy (IE) of a chemical species may reveal its structural information. Fig. 1 shows the photoionization efficiency spectra of DMS and the products of F<sub>2</sub> + DMS reaction. The *m/z* = 80 product corresponds to a formula of C<sub>2</sub>H<sub>5</sub>SF which has two likely structures, CH<sub>2</sub>=S(F)-CH<sub>3</sub> and CH<sub>2</sub>F-S-CH<sub>3</sub>. The computed adiabatic ionization energies are 8.59 eV for CH<sub>2</sub>=S(F)-CH<sub>3</sub>, 8.70 eV for DMS, and 9.09 eV for CH<sub>2</sub>F-S-CH<sub>3</sub>.<sup>26</sup> It is clear that the IE of CH<sub>2</sub>F-S-CH<sub>3</sub> is too

high to match the observation; the reaction product of *m/z* = 80 can be reasonably assigned to the CH<sub>2</sub>=S(F)-CH<sub>3</sub> structure. For the product of *m/z* = 81, its ionization threshold is distinctive, about 0.9 eV lower than that of DMS. The most reasonable assignment for this mass is a structure corresponding to CH<sub>3</sub>-S(F)-CH<sub>3</sub> with calculated vertical IE of 7.89 eV.<sup>26</sup> Baker *et al.*<sup>39</sup> also observed this species with photoelectron spectroscopy (PES) but they missed the main reaction product of CH<sub>2</sub>=S(F)-CH<sub>3</sub>. As shown in Fig. 1, the ionization thresholds of CH<sub>2</sub>=S(F)-CH<sub>3</sub> and DMS are very similar. Thus, in the PES detection,<sup>39</sup> the observation of the major reaction product (CH<sub>2</sub>=S(F)-CH<sub>3</sub>) was fully obscured by the intense peak of the DMS reactant.

### 3.2 First barrierless reaction between closed-shell reactants

The molecular beam method is very useful to study the collision energy dependence of elementary processes. When we reduced the collision energy of the F<sub>2</sub> + DMS reaction,<sup>26,27</sup> to our surprise, we found that the reaction probability of (R1) increased. For a reaction with a potential energy barrier, a certain amount of energy is needed to overcome the barrier (except tunneling which is a different issue) and energy in various forms (translational, rotational, vibrational, *etc.*) may have different efficiency. But here we have a different situation: the F<sub>2</sub> + DMS reaction does not require any energy, indicating this reaction has no barrier! Later investigations of the F<sub>2</sub> + DMDS reaction<sup>28</sup> indicate that the F<sub>2</sub> + DMDS reaction is also barrierless.

To better understand the unusual reactivity between F<sub>2</sub> and DMS/DMDS, *ab initio* calculations have been performed.<sup>26–28</sup> The employed computational methods include CASPT2, QCISD(T), and CCSD(T).<sup>40</sup> In addition, various sizes of basis sets have been used to ensure that the computational results are adequate. Fig. 2 shows the 2-dimensional (2D) potential energy surface near the entrance valley and the reaction intermediate (INT) of the F<sub>2</sub> + DMS reaction. Because the structure of the (CH<sub>3</sub>)<sub>2</sub>S moiety of INT is very similar to the reactant structure, the 2D rigid scan (other degrees of freedom are frozen) of the potential energy surface is almost identical to the relax scan (other degrees of freedom are optimized). A barrier (TS1, a saddle point with only one imaginary vibrational frequency) has been located in between the van der Waals entrance well (VDW) and INT. But the potential energy surface is very flat near TS1 and the energy of TS1 is about 2.5 kcal mol<sup>-1</sup> lower than that of the separated reactants (S-F distance ∼ 10 Å).

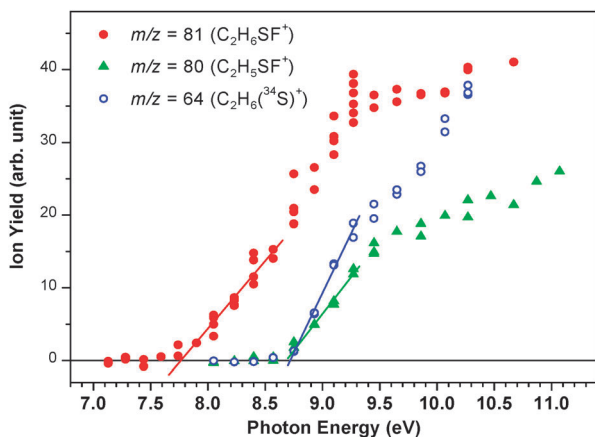


**Fig. 1** Photoionization efficiency spectra of DMS and the products (*m/z* = 80, 81) of the F<sub>2</sub> + DMS reaction at ∼8 kcal mol<sup>-1</sup> collision energy. A minor isotope of sulfur, <sup>34</sup>S (natural abundance ratio: <sup>34</sup>S/<sup>32</sup>S = 0.043/0.95), was chosen when detecting DMS (*m/z* = 64) simply because the count rate at *m/z* = 62 was very high, close to the saturation level of our detector (10<sup>6</sup> counts s<sup>-1</sup>).

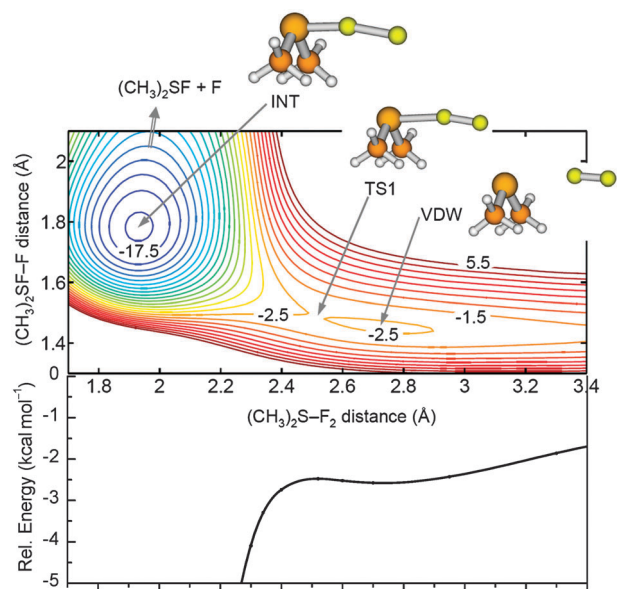


**Fig. 2** CASPT2 potential energy surface for the entrance valley and INT of the  $F_2 + \text{DMS}$  reaction. The numbers indicate the potential energies relative to the separated reactants in  $\text{kcal mol}^{-1}$ . The contour spacing is  $1 \text{ kcal mol}^{-1}$ . The inactive geometrical variables are fixed at the optimized TS1 structure. The potential energy profile along the minimum energy path near TS1 and VDW is depicted below the contour plot. This figure is modified from the results of ref. 27.

In addition, this barrier *disappears* at the CCSD(T) and QCISD(T) levels of calculation.<sup>27</sup>

Both experimental and theoretical results<sup>26–28</sup> of the  $F_2 + \text{DMS}/\text{DMDS}$  reactions indicate that these reactions are barrierless. For barrierless reactions, a capture theory<sup>41,42</sup> can often be applied that considers only the entrance part of the potential energy surface. Although most reported barrierless reactions are reactions between ions and molecules or those involving open-shell radicals,<sup>43,44</sup> some analogous reactions may help us to better understand the results of the  $F_2 + \text{DMS}/\text{DMDS}$  reactions. A series of low temperature studies on the reactions of  $O(^3P) + \text{alkenes}$  (propene and butenes) show that the reaction rate constants increase with decreasing temperature.<sup>45</sup> The minimum energy curve of the  $F_2 + \text{DMS}$  reaction (Fig. 2) looks similar to those of the  $O(^3P) + \text{alkene}$  reactions:<sup>45</sup> there is a “submerged” barrier corresponding to a maximum along the minimum energy path between the shallow minimum associated with a van der Waals complex and the more stable reaction intermediate (or products). A “two transition state” model<sup>46,47</sup> has been employed to describe reactions of this type. For the  $F_2 + \text{DMS}$  reaction, because the submerged barrier (TS1) is even lower in energy, one may expect that the reaction rate constant will reach the capture limit at low temperatures. This hypothesis, however, requires further evidence from both experiment and theory. The lowest collision energy in our previous study<sup>26–28</sup> was about  $1 \text{ kcal mol}^{-1}$ . It will be very interesting if the study can be extended to lower collision energies or at low temperatures.

After passing over the submerged barrier TS1, an intermediate INT is formed in the  $F_2 + \text{DMS}$  reaction. As mentioned above, an important feature of INT is that the  $S(\text{CH}_3)_2$  moiety is very similar in structure to the DMS reactant. Fig. 3 shows the three

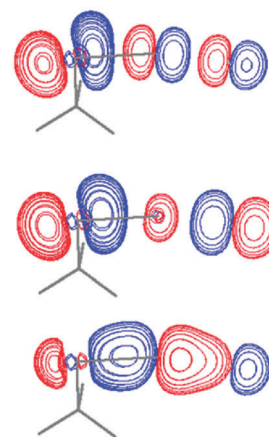


**Fig. 3** Frontier molecular orbitals of INT of the  $F_2 + \text{DMS}$  reaction calculated with the CASSCF method. As seen in this figure, the orbitals involved are mainly  $3p_z$  on S (left in the figure),  $\sigma/\sigma^*$  on  $F_2$ .

most important (frontier) molecular orbitals (MO) of INT. In Fig. 3, we can see that the  $3p_z$  (S) and  $\sigma/\sigma^*$  ( $F_2$ ) orbitals are involved and the resulting molecular orbitals can be described as bonding, non-bonding and anti-bonding among these three atoms. In the MO point of view, there are mainly 4 electrons involved: 2 from the lone pair of S, 2 from the sigma bond of  $F_2$ , a picture of “3-center-4-electron bond”.<sup>48,49</sup> Because the involved orbital at S is a lone pair, other chemical bonds are almost unperturbed, resulting in minor structural change in the  $S(\text{CH}_3)_2$  moiety.

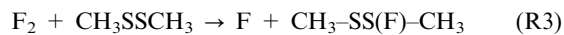
There are two decay channels for INT. A simple fission of the  $F\text{--}F\text{S}(\text{CH}_3)_2$  bond leads to  $F + \text{CH}_3\text{--}S(\text{F})\text{--}CH_3$  (R2), which is moderately endothermic. The other path may be described as the outer F atom attacks one H atom at one of the methyl groups, resulting in HF formation (R1).<sup>26,27</sup> As will be shown later, the products of an analogous reaction,  $F_2 + \text{CH}_3\text{SSCH}_3$ ,<sup>28</sup> provide further evidence for this picture.

The product angular distribution provides information about the reaction time scale. If the reaction time is substantially longer than one rotation period of the reaction complex, a forward-backward symmetric angular distribution is expected. This type of angular distribution arises from losing directional memory due to rotation while remembering the plane of rotation because of conservation of angular momentum. As a result, the rotation period can be used as an “internal clock” for reactive scattering.<sup>50</sup> With the moment of inertia of INT and the range of the collision energies, the rotation period of INT can be estimated to be a couple of picoseconds for the  $F_2 + \text{DMS}$  reaction. The observed products exhibit forward-biased angular distributions,<sup>27</sup> indicating that the reaction is faster than rotation. This result suggests that although the existence of INT may slow down the reaction, INT is not stable enough to support a lifetime longer than a couple of picoseconds.

### 3.3 Confirm the reaction mechanism by the $F_2 + \text{CH}_3\text{SSCH}_3$ reaction

Similar to the  $F_2 + \text{DMS}$  reaction, a product channel producing a F atom and a fluoro radical (R3) was observed in the reaction of  $F_2 + \text{DMDS}$  at collision energy higher than  $4.3 \pm 0.4 \text{ kcal mol}^{-1}$ .

However, in contrary to the  $F_2 + DMS$  reaction, no HF product channel (R4) could be found in the crossed beam reaction of  $F_2 + DMDS$ . Instead, the main product channel produces 2  $CH_3SF$  molecules (R5). As mentioned above, significant reaction signal of (R5) has also been observed at collision energies as low as  $1\text{ kcal mol}^{-1}$ .<sup>28</sup>



A similar intermediate structure with a nearly linear F–F–S bonding has been found theoretically for the  $F_2 + DMDS$  reaction and, again, it can be formed without a barrier. We may consider three possible decay channels from this intermediate: (i) breaking of the F–F bond leads to F atom production (R3); (ii) the outer F atom attacks one H atom leading to HF formation (R4); and (iii) the outer F atom attacks the other S atom leading to  $CH_3SF + CH_3SF$  (R5). With the experimental results,<sup>28</sup> we can conclude that the F–F bond fission of the intermediate has an energy threshold and the outer F atom preferably attacks the S atom, not an H atom.

In brief summary, barrierless reactions of molecular fluorine with DMS and DMDS have been investigated with crossed molecular beam experiments and *ab initio* calculations.<sup>26–28</sup> While previously reported molecule–molecule reactions<sup>12–19</sup> exhibit significant energy thresholds, these two reactions show substantial reaction probability even at low energies. One may expect that there exist other types of reactions which are barrierless as well, for example, those mentioned by Turnipseed and Birks.<sup>37</sup> However, although it needs further investigations,  $F_2$  seems to be a unique reactant in this regard. Nonetheless, to explore such reactions at extremely low temperatures will be a new challenge. For such molecule–molecule reactions, comparison between low temperature rate measurements and high level theories would advance our understanding on chemical reactivity.

#### 4. $F_2 +$ alkene reactions

Miller *et al.*<sup>51</sup> suggested that the reaction of molecular fluorine and olefin proceeds *via* an initiation step with production of a fluorine atom and a free fluoro-radical. However, this reaction mechanism was not universally accepted due to lack of further evidence. Hauge *et al.*<sup>52</sup> suggested that the activation energies of  $F_2$  reactions with the following molecules are in the order of (propylene  $\approx$  butadiene  $\approx$  cyclohexene  $<$  ethylene  $\approx$  allene  $<$  benzene, alkane, alkyne). These earlier studies provide some qualitative observations. More quantitative and definitive information is required to understand the dynamics of the  $F_2 +$  alkene reactions.

For  $F_2$  reaction with the simplest alkene  $C_2H_4$ , three product channels are possible (the reaction enthalpies are from CCSD(T) calculations<sup>29</sup>).



Early studies<sup>53–56</sup> under matrix-isolation conditions reported detection of the reaction products of  $HF + C_2H_3F$  (R7) and  $C_2H_4F_2$  (R8) by means of Fourier-transform infrared (FT-IR) spectroscopy, but recent crossed molecular beam studies<sup>29</sup> on the same reaction only observed  $F + C_2H_4F$  (R6) as the products. This disparity may be accounted for by the cage effect which is common in condensed phases, but absent in crossed beam experiments. In the matrix-isolation conditions, it is very likely that the F atom product is trapped in the same cage and recombines with the radical site of  $C_2H_4F$ , forming vibrationally excited  $C_2H_4F_2$ . The excited  $C_2H_4F_2$  may either be stabilized or decompose to  $HF + C_2H_3F$ .

The product angular and translational energy distributions may be used to learn the reaction dynamics. Fig. 4 shows a product velocity contour map of the  $C_2H_4F$  product of (R6) at  $6.6\text{ kcal mol}^{-1}$  collision energy. Such a plot shows the distribution of the recoil velocity vectors in the center-of-mass frame. If we follow the motion of the  $C_2H_4$  moiety, it recoils into the backward hemisphere after reaction with  $F_2$ . This product angular distribution is consistent with a picture of a typical rebound reaction with a barrier<sup>2</sup> ( $5.5\text{ kcal mol}^{-1}$  for this reaction; see below). In such a reaction mechanism, collisions at small impact parameters have sufficient collision energy along the line-of-centers, leading to reactive scattering into the backward directions; collisions at large impact parameters cannot surmount the barrier to reaction. More precisely speaking, the reaction probability decreases at large impact parameters where the centrifugal barriers are higher. The strongly backward distribution of the product also indicates that the direction of the recoil force is opposite to the incoming velocity, which is consistent with the calculated potential energy gradient at the transition state<sup>29</sup> (the transition state has a nearly linear F–F–C structure and the F atom product recoils along the F–F bond direction). Furthermore, the kinetic energy release of the products is only  $\sim 28\%$  of the

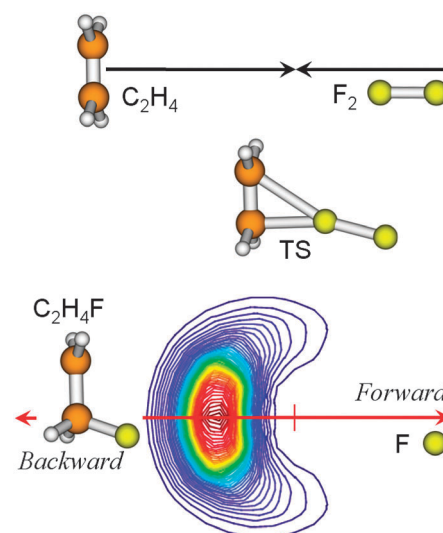
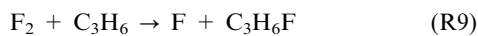


**Fig. 4** Schematic structures of the reactants, transition state (TS) and products of  $F_2 + C_2H_4 \rightarrow C_2H_4F + F$  reaction.<sup>29</sup> The velocity-flux map of the  $C_2H_4F$  product<sup>29</sup> is also shown (collision energy =  $6.6\text{ kcal mol}^{-1}$ ). By conservation of linear momentum, the F atom product is scattered into the opposite direction of the  $C_2H_4F$  product.

available energy,<sup>29</sup> indicating significant internal excitation ( $\sim 72\%$  of the available energy) of the C<sub>2</sub>H<sub>4</sub>F product. This observation is consistent with the calculated geometry<sup>29</sup> of the transition state which is more similar to the reactant structure than to the product structure. In this case, it can be classified as an earlier barrier according to the Polanyi rule<sup>57</sup> which would predict more internal excitation rather than translational excitation for the product.

One of the motivations to study the reactions of F<sub>2</sub> with alkenes larger than C<sub>2</sub>H<sub>4</sub> was to search for a direct HF formation channel. The idea is based on the F<sub>2</sub> + C<sub>2</sub>H<sub>4</sub> reaction mechanism and the molecular geometries: when the F<sub>2</sub> attacks the  $\pi$ -bond of C<sub>2</sub>H<sub>4</sub>, the four H atoms on the C<sub>2</sub>H<sub>4</sub> are all quite far away from the F atoms.<sup>29</sup> As a result, the probability of HF formation would be very small. This probability might be enhanced for a methyl-substituted ethylene which is a non-planar molecule and the H atoms of the methyl group may have a chance to be closer to the F atoms. Whether the HF channel exists in the F<sub>2</sub> + alkene reactions may provide important mechanistic information regarding the fluorination of olefins.

We have searched for both F and HF product channels in crossed molecular beam experiments of F<sub>2</sub> reactions with C<sub>3</sub>H<sub>6</sub> and isomers of C<sub>4</sub>H<sub>8</sub>. Still, the HF formation channels were not observed; the observed reactions are (R9)<sup>30</sup> and (R10).<sup>31</sup> In the regard of the product angular and translational energy distributions, the results of the F<sub>2</sub> + C<sub>3</sub>H<sub>6</sub> reaction (R9)<sup>30</sup> very much resemble those of the F<sub>2</sub> + C<sub>2</sub>H<sub>4</sub> reaction (R6).<sup>29</sup>



## 5. Comparison between the F<sub>2</sub> + organosulfur reactions and F<sub>2</sub> + alkene reactions

If we compare the F<sub>2</sub> + organosulfur reactions<sup>26–28</sup> and the F<sub>2</sub> + alkene reactions,<sup>29–31</sup> a common feature is that the transition states all have a nearly linear F–F–X structure (X denotes S atom or C=C  $\pi$ -bond). This linear structure is consistent with a picture of frontier MO which involves  $\sigma/\sigma^*$  orbitals of F<sub>2</sub> and a doubly occupied orbital on X ( $n_{\text{S}}$  or  $\pi_{\text{CC}}$ ); a linear structure would have the best overlap of the involved MO. However, in the organosulfur case there is an intermediate and a simple F–FX bond fission is endothermic with respect to the reactants, such that the outer F atom is bound and may interact with other moieties of the intermediates, like an H atom on the methyl group or another S atom. Such an intermediate is absent in the F<sub>2</sub> + alkene case and a simple F–FX bond fission is exothermic; since the outer F atom is not bound at all, it would just fly away after passing the transition state.

## 6. Problem of reaction thresholds

The F<sub>2</sub> reactions with simple alkenes (*e.g.*, C<sub>2</sub>H<sub>4</sub> or C<sub>3</sub>H<sub>6</sub>) exhibit thresholds in energy. For the F<sub>2</sub> + C<sub>2</sub>H<sub>4</sub> reaction, crossed beam results give a threshold of  $5.5 \pm 0.5$  kcal mol<sup>-1</sup> in collision energy,<sup>29</sup> a kinetic study reported an activation energy of 4.6 kcal mol<sup>-1</sup>;<sup>58</sup> frequency dependence of IR excitation under matrix-isolation conditions indicates the reaction threshold is 5.4 kcal mol<sup>-1</sup> or less.<sup>53–56</sup> Although this

reaction (R6) is relatively simple—a single transition state separates the products from the reactants—our CCSD(T) calculations<sup>29</sup> give a potential energy barrier of 7.1 kcal mol<sup>-1</sup>, substantially higher than the experimental threshold (or activation energy). There are two possibilities for this disagreement: (i) the experimental threshold may be lowered by internal excitations of the reactants, and (ii) the theoretical barrier height is not accurate enough.

For possibility (i), the rotational and vibrational excitation of the reactants (electronic excitation is impossible in this case), especially the F<sub>2</sub> vibration (894 cm<sup>-1</sup>), may contribute to the experimental activation energy which has been measured to be 4.6 kcal mol<sup>-1</sup> in a temperature range of 300 to 430 K.<sup>58</sup> Such a temperature range corresponds to a variation of population ratio from 1.4 to 5% for F<sub>2</sub>(*v* = 1)/F<sub>2</sub>(*v* = 0). But it is quite different in the molecular beam conditions. First we should not worry about rotational excitations since our molecular beams were very cold rotationally. Second, much lower temperatures (150/300 K) were used for the F<sub>2</sub> beam nozzle and the effect of the vibrational excitations of the reactants has been checked by varying the nozzle temperatures of the molecular beams; the results<sup>29</sup> indicate that this effect is quite minor and will not change the threshold by a significant amount.

On the other hand, it is not clear for possibility (ii). Initially we suspected that our level of theory is not high enough. However, a very rigorous computation by Feng and Allen<sup>59</sup> still gives a potential energy barrier of 8.0 kcal mol<sup>-1</sup>. Their work<sup>59</sup> used a focal point approach to converge toward the *ab initio* limit; explicit computations were executed with basis sets as large as aug-cc-pV5Z and correlation treatments as extensive as coupled cluster through full triples with a perturbative inclusion of quadruple excitations CCSDT(Q)—the highest level of computation currently feasible.

If we believe both experiment and theory have an error bar of about 1 kcal mol<sup>-1</sup>, it is hard to imagine how a reaction can take place if the total energy is below the potential energy barrier. It is expected that tunneling will have little contribution to this reaction since it does not involve light atom transfer. Thus, the barrier for F<sub>2</sub> + C<sub>2</sub>H<sub>4</sub> reaction may pose a general problem to be resolved between theory and experiment.

While theory and experiment do not match very well in the barrier height of the F<sub>2</sub> + C<sub>2</sub>H<sub>4</sub> reaction,<sup>29,59</sup> the reaction of F<sub>2</sub> + C<sub>3</sub>H<sub>6</sub> becomes an important testing case. Remarkably, the measured threshold ( $2.4 \pm 0.3$  kcal mol<sup>-1</sup>)<sup>30</sup> is still  $\sim 2$  kcal mol<sup>-1</sup> lower than the corresponding barrier heights calculated with the CCSD(T) method.<sup>30,31</sup> In Fig. 5, we compare the calculated potential energy barrier heights and the experimental thresholds in collision energy for F<sub>2</sub> reactions with a few simple alkenes. In addition to the discrepancies between theory and experiment, it is interesting to see that the theoretical barrier heights for the F<sub>2</sub> reactions with *cis*-, *trans*- and *iso*-butenes are very low, less than 1 kcal mol<sup>-1</sup>. Compared with the F<sub>2</sub> + 1-C<sub>4</sub>H<sub>8</sub> reaction, these theoretical results suggest that double methyl substitution at the C=C double bond would efficiently reduce the reaction barriers with F<sub>2</sub>. Currently there are no experimental data available for the F<sub>2</sub> + C<sub>4</sub>H<sub>8</sub> reaction thresholds. It would be very interesting to see if the theoretical prediction is valid or not.

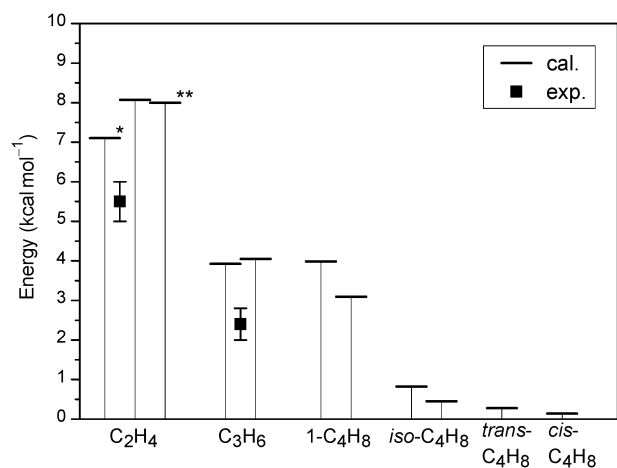


**Fig. 5** Comparison of the calculated potential energy barriers ( $\Delta ZPE$  included) and the experimental thresholds in collision energy<sup>29,30</sup> for  $F_2$  reactions with simple alkenes. The calculated data marked with \* are from ref. 29, \*\* from ref. 59, and the rest are from ref. 31. For an asymmetric  $C=C$  double bond, there are two transition state structures (see ref. 31 for details).

## 7. Summary

The  $F_2$  reactions with DMS, DMDS,  $C_2H_4$ ,  $C_3H_6$ , and  $C_4H_8$  have been investigated with crossed molecular beam methods. Nascent products have been identified with electron-impact and vacuum UV-photoionization mass spectrometry. High level *ab initio* calculations have been performed to interpret the experimental observations and to draw a picture of the reaction mechanisms. For the  $F_2$  reactions with DMS and DMDS, a short-lived intermediate of nearly linear F–F–S structure can be formed without a potential energy barrier. Kinetic measurements at extremely low temperatures will reveal more insights into these intriguing barrierless reactions and to confirm the theoretical findings.

For the  $F_2$  reactions with  $C_2H_4$ ,  $C_3H_6$  and  $C_4H_8$ , there is a single barrier separating the products from the reactants and the only observed product channel is the F atom formation. The product angular and translational energy distributions are consistent with a typical rebound reaction mechanism with an early barrier, which is further supported by the theoretical calculations. However, the theoretical barrier heights of the  $F_2$  reactions with  $C_2H_4$  and  $C_3H_6$  are about  $2 \text{ kcal mol}^{-1}$  too high, compared with the experimental reaction thresholds in collision energy. The theoretical prediction that the  $F_2$  reactions with double methyl substituted ethylene are almost barrierless is yet to be confirmed experimentally.

For low energy molecule–molecule reactions, it seems that  $F_2$  is a unique reactant. We have tried  $O_3 + DMS$  and  $Cl_2 + DMS$  reactions but did not observe any reactive signal under conditions similar to the  $F_2 + DMS$  reaction. The HOMO–LUMO gap of a  $F_2$  molecule was found to decrease very significantly at a slightly elongated bond length that may be an important factor in its reactivity. More molecule–molecule reactions deserve investigations in more depth, both experimentally and theoretically.

## 8. Appendix: CW vs. pulsed beam

In principle, the experiments can be performed in either continuous (CW) mode or pulsed mode. At first glance, the CW mode seems simpler. However, we adapted the pulsed mode in our previous studies for the following reason. Consider a reaction  $A + B \rightarrow P$ . The gas consumption is proportional to the gas density ( $n$ ) and the fraction of on-time ( $f$ ) of a molecular beam ( $f = 1$  for a CW beam). The product signal per integration time ( $N_P$ ) is proportional to the densities of both reactants and the effective duty cycle ( $w$ ), along with other parameters like the reaction volume which are the same for both CW mode and pulsed mode.

$$N_P = \alpha n_A n_B w \quad (1)$$

where the proportional constant  $\alpha$  represents the overall effect of other parameters. For a CW experiment, a pseudo-random chopper may be used to resolve the time-of-flight of the scattered product. Such a chopper may have an effective duty cycle of about 0.5. For a pulsed experiment,  $w = \min(f_A, f_B)$ . If the gas density is mainly limited by the pumping speed of the source chamber, we will have  $\eta f = C$ ,  $C$  is a constant denoting the pumping speed. A simple deduction leads to

$$N_P^{CW} = \alpha n_A n_B w = \alpha \frac{C_A C_B}{1} 0.5 = 0.5 \alpha C_A C_B \quad (2)$$

$$N_P^{Pulsed} = \alpha n_A n_B w = \alpha \frac{C_A C_B}{f} f = \alpha \frac{C_A C_B}{f} \quad (3)$$

For simplicity, we let  $f_A = f_B = f$  in the pulsed mode. For a high speed pulsed valve (Even–Lavie valve),<sup>60</sup> the pulse width can be shorter than  $20 \mu\text{s}$  and the repetition rate can be as high as 1000 Hz. In the experiment, we reduced the repetition rate to 200 Hz for a more suitable (longer lifetime of the valve sealing gasket) operation and the calculated  $f$  value would be about  $2 \times 10^{-3}$ , assuming the density is only limited by the pumping speed. The maximum enhancement factor of the pulsed mode over the CW mode is then estimated to be  $1/(0.5f) = 1000$ . The enhancement factor in a practical experiment may be smaller because the value of  $\eta f$  may not have reached the pumping-speed limit. An educated guess of a practical enhancement factor may be about 100.

## Acknowledgements

This work was supported by Academia Sinica and the National Science Council of Taiwan (NSC 100-2113-M-001-008-MY3). The author thanks Prof. Yuan T. Lee for valuable comments.

## Notes and references

- 1 Y. T. Lee, *Science*, 1987, **236**, 793.
- 2 R. D. Levine and R. B. Bernstein, *Molecular Reaction Dynamics and Chemical Reactivity*, Oxford University Press, New York, 1987.
- 3 *Modern Trends in Chemical Reaction Dynamics: Experiment and Theory*, ed. X. Yang and K. Liu, World Scientific, Singapore, 2004.
- 4 P. Casavecchia, *Rep. Prog. Phys.*, 2000, **63**, 355.
- 5 K. Liu, *Annu. Rev. Phys. Chem.*, 2001, **52**, 139.
- 6 K. Liu, *Int. Rev. Phys. Chem.*, 2001, **20**, 189.
- 7 R. I. Kaiser, *Chem. Rev. (Washington, DC)*, 2002, **102**, 1309.

- 8 C. Murray and A. J. Orr-Ewing, *Int. Rev. Phys. Chem.*, 2004, **23**, 435.
- 9 M. N. R. Ashfold, N. H. Nahler, A. J. Orr-Ewing, O. P. J. Vieuxmarie, R. L. Toomes, T. N. Kitsopoulos, I. A. Garcia, D. A. Chestakov, S.-M. Wu and D. H. Parker, *Phys. Chem. Chem. Phys.*, 2006, **8**, 26.
- 10 X. Yang, *Phys. Chem. Chem. Phys.*, 2006, **8**, 205.
- 11 X. Yang, *Int. Rev. Phys. Chem.*, 2005, **24**, 37.
- 12 J. M. Farrar and Y. T. Lee, *J. Am. Chem. Soc.*, 1974, **96**, 7570.
- 13 J. M. Farrar and Y. T. Lee, *J. Chem. Phys.*, 1975, **63**, 3639.
- 14 M. J. Coggiola, J. J. Valentini and Y. T. Lee, *Int. J. Chem. Kinet.*, 1976, **8**, 605.
- 15 J. J. Valentini, M. J. Coggiola and Y. T. Lee, *J. Am. Chem. Soc.*, 1976, **98**, 853.
- 16 J. J. Valentini, M. J. Coggiola and Y. T. Lee, *Faraday Discuss. Chem. Soc.*, 1977, **62**, 232.
- 17 C. C. Kahler and Y. T. Lee, *J. Chem. Phys.*, 1980, **73**, 5122.
- 18 J. M. Farrar and Y. T. Lee, *J. Chem. Phys.*, 1976, **65**, 1414.
- 19 J. R. Grover, Y. Wen, Y. T. Lee and K. Shobatake, *J. Chem. Phys.*, 1988, **89**, 938.
- 20 D. Patel-Misra, D. G. Sauter and P. J. Dagdigian, *J. Chem. Phys.*, 1991, **95**, 955.
- 21 J. H. Choi, *Int. Rev. Phys. Chem.*, 2006, **25**, 613.
- 22 N. Balucani, F. Leonori, A. Bergeat, R. Petrucci and P. Casavecchia, *Phys. Chem. Chem. Phys.*, 2011, **13**, 8322.
- 23 F. Leonori, N. Balucani, G. Capozza, E. Segoloni, D. Stranges and P. Casavecchia, *Phys. Chem. Chem. Phys.*, 2007, **9**, 1307.
- 24 P. Casavecchia, F. Leonori, N. Balucani, R. Petrucci, G. Capozza and E. Segoloni, *Phys. Chem. Chem. Phys.*, 2009, **11**, 46.
- 25 R. I. Kaiser, W. Sun, A. G. Suits and Y. T. Lee, *J. Chem. Phys.*, 1997, **107**, 8713.
- 26 Y.-J. Lu, L. Lee, J.-W. Pan, H. A. Witek and J. J. Lin, *J. Chem. Phys.*, 2007, **127**, 101101.
- 27 Y.-J. Lu, L. Lee, J.-W. Pan, T. Xie, H. A. Witek and J. J. Lin, *J. Chem. Phys.*, 2008, **128**, 104317.
- 28 H.-C. Shao, T. Xie, Y.-J. Lu, C.-H. Chang, J.-W. Pan and J. J. Lin, *J. Chem. Phys.*, 2009, **130**, 014301.
- 29 Y.-J. Lu, T. Xie, J.-W. Fang, H.-C. Shao and J. J. Lin, *J. Chem. Phys.*, 2008, **128**, 184302.
- 30 J.-W. Fang, T. Xie, H.-Y. Chen, Y.-J. Lu, Y. T. Lee and J. J. Lin, *J. Phys. Chem. A*, 2009, **113**, 4381.
- 31 Z.-Q. Li, C.-H. Tsai, A. F. Chen, Y.-J. Lu and J. J. Lin, *Chem. Phys. Lett.*, 2011, **510**, 42.
- 32 J. J. Lin, D. W. Hwang, S. Harich, Y. T. Lee and X. Yang, *Rev. Sci. Instrum.*, 1998, **69**, 1642.
- 33 Y. T. Lee, J. D. McDonald, P. R. Lebreton and D. R. Herschbach, *Rev. Sci. Instrum.*, 1969, **40**, 1402.
- 34 J. J. Lin, Y. Chen, Y. Y. Lee, Y. T. Lee and X. Yang, *Chem. Phys. Lett.*, 2002, **361**, 374.
- 35 S. H. Lee, J. J. Lin and Y. T. Lee, *J. Electron Spectrosc. Relat. Phenom.*, 2005, **144**, 135.
- 36 X. Yang, D. A. Blank, J. Lin, A. G. Suits, Y. T. Lee and A. M. Wodtke, *Rev. Sci. Instrum.*, 1997, **68**, 3317.
- 37 A. A. Turnipseed and J. W. Birks, *J. Phys. Chem.*, 1991, **95**, 6569.
- 38 <http://kinetics.nist.gov>.
- 39 J. Baker, V. A. Butcher, J. M. Dyke and E. P. F. Lee, *J. Phys. Chem.*, 1995, **99**, 10147.
- 40 CASPT2 is a complete-active-space self-consistent-field calculation with the second-order multireference perturbation theory corrections. QCISD(T) is a calculation method of Quadratic Configuration Interaction with Single and Double and Perturbative Triple excitations. CCSD(T) is a calculation of Coupled-Cluster with Single and Double and Perturbative Triple excitations. For the F<sub>2</sub> + DMS/DMDS reaction systems, the use of a multireference method such as CASPT2 is important to describe the full reaction paths.
- 41 D. C. Clary, *Annu. Rev. Phys. Chem.*, 1990, **41**, 61.
- 42 J. Troe, *J. Chem. Soc., Faraday Trans.*, 1994, **90**, 2303.
- 43 D. C. Clary, *Proc. Natl. Acad. Sci. U. S. A.*, 2008, **102**, 6648.
- 44 B. Hansmann and B. Abel, *ChemPhysChem*, 2007, **8**, 343.
- 45 H. Sabbah, L. Biennier, I. R. Sims, Y. Georgievskii, S. J. Klippenstein and I. W. M. Smith, *Science*, 2007, **317**, 102.
- 46 Y. Georgievskii and S. J. Klippenstein, *J. Phys. Chem. A*, 2007, **111**, 3802.
- 47 S. J. Klippenstein, Y. Georgievskii and L. B. Harding, *Phys. Chem. Chem. Phys.*, 2006, **8**, 1133.
- 48 C. A. Ramsden, *Chem. Soc. Rev.*, 1994, **23**, 111.
- 49 J. M. Molina and J. A. Dobado, *Theor. Chem. Acc.*, 2001, **105**, 328.
- 50 G. A. Fisk, J. D. McDonald and D. R. Herschbach, *Faraday Discuss. Chem. Soc.*, 1967, **44**, 228.
- 51 (a) W. T. Miller Jr. and A. L. Dittman, *J. Am. Chem. Soc.*, 1956, **78**, 2793; (b) W. T. Miller Jr., S. D. Koch Jr. and F. W. McLafferty, *J. Am. Chem. Soc.*, 1956, **78**, 4992; (c) W. T. Miller Jr. and S. D. Koch Jr., *J. Am. Chem. Soc.*, 1956, **79**, 3084.
- 52 R. H. Hauge, S. Gransden, J. L.-F. Wang and J. L. Margrave, *J. Am. Chem. Soc.*, 1979, **101**, 6950.
- 53 H. Frei, L. Fredin and G. C. Pimentel, *J. Chem. Phys.*, 1981, **74**, 397.
- 54 H. Frei and G. C. Pimentel, *J. Chem. Phys.*, 1983, **78**, 3698.
- 55 H. Frei, *J. Chem. Phys.*, 1983, **79**, 748.
- 56 H. Frei and G. C. Pimentel, *Annu. Rev. Phys. Chem.*, 1985, **36**, 491.
- 57 J. C. Polanyi, *Acc. Chem. Res.*, 1972, **5**, 161.
- 58 G. A. Kapralova, A. M. Chaikin and A. E. Shilov, *Kinet. Katal.*, 1967, **8**, 421.
- 59 H. Feng and W. D. Allen, *J. Chem. Phys.*, 2010, **132**, 094304.
- 60 U. Even, J. Jortner, D. Noy and N. Lavie, *J. Chem. Phys.*, 2000, **112**, 8068.